1973
Seis Soc Amer Bull
v63

...ogradskii (1963). A stu...
...ck-samples under con...
...glish Transl.) 8, 728-...
...Res. 65, 757-766. ...
...eol. Soc. Am., Speci...
...J. Geophys. Res. 70, ...
...in single crystals, J...
...a two phase material. ...
effective stress, and fun...
...38.

...OLOGY AND
...SCIENCES (W. S. B.)
...STITUTE OF TECHNOLOGY
...IFORNIA 91109

USE OF REFLECTION PHASES ON MICROEARTHQUAKE SEISMOGRAMS TO MAP AN UNUSUAL DISCONTINUITY BENEATH THE RIO GRANDE RIFT

BY ALLAN R. SANFORD, ÖMER ALPTEKIN, AND TOUSSON R. TOPPOZADA

ABSTRACT

Microearthquake seismograms recorded by stations located in or bordering the Rio Grande rift near Socorro, New Mexico, frequently have two sharp impulsive phases following direct *S*. These phases have been identified as S_xP and S_xS reflections from a sharp discontinuity that has a depth beneath Socorro of 18 km and dips northward at an angle near 6° for a distance of 30 km. Farther north, the dip steepens so that at a distance of 60 km from Socorro the depth is about 30 km. Ratios of S_xP to S_xS amplitudes in conjunction with plane-wave reflection theory indicate a zone of very low rigidity beneath the discontinuity. Large S_xS amplitudes are believed to be the result of the large velocity contrast across the discontinuity and a fault mechanism that radiates more *S*-wave energy downward than outward from the focus.

INTRODUCTION

...is paper describes the use of reflection phases on microearthquake seismograms to ...mine the depth and characteristics of a velocity discontinuity beneath the Rio ...de rift near Socorro, New Mexico. In an earlier paper on this subject, Sanford and ... (1965) interpreted these reflected phases as S_xP and S_xS reflections from a dis...uity at a depth of 18 km. Data presented here remove any uncertainty about this ...retation. In addition, the discontinuity is shown to dip northward from Socorro ...to be underlain by material of very low rigidity. The large amplitudes of the re...d phases are explained by a large *S*-phase velocity contrast across the discontinuity ...eferential downward radiation of *S*-wave energy from the earthquake foci.

THE RIO GRANDE RIFT

...orro, New Mexico is located within a major tectonic structure known as the Rio ...de rift. In detail, the rift is a series of linked structural depressions, with raised ...s, extending from southern New Mexico into central Colorado (Kelley, 1952, ...Chapin, 1971). In southern Colorado and northern New Mexico, the rift penetrates ...uthern Rocky Mountains, and in southern New Mexico it merges in a complex ...known way with the Basin and Range Province (index map, Figure 1). The rift ...be considered a long narrow northward extension of the Basin and Range Province. ...e graben structures that comprise the rift began forming about 20 m.y. ago. In the ...querque-Socorro segment of the rift, differential vertical movements between basins ...ordering highlands computed from gravity anomalies range from 3 km at Socorro ...km at Albuquerque (Joesting, Case, and Cordell, 1961; Geddes, 1963; Sanford, ... Although total movement at Socorro is much less than at Albuquerque, Denny ...) believed that the mountains immediately west of Socorro are intergraben horsts ...very young age, perhaps post-Pliocene. This would indicate rates of vertical move...in the Socorro area of 1 to 3 mm/year. Evidence that this differential vertical move-

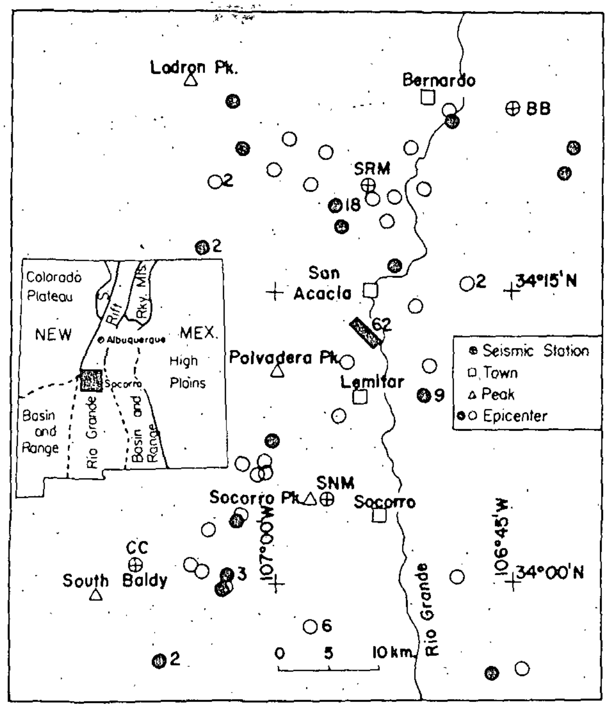

FIG. 1. Map showing location of seismograph stations and epicenters for microearthquakes occurring from July 1, 1969 through June 30, 1970. The solid circles and rectangle indicate good earthquake locations; the open circles indicate fair locations. Numbers are used when more than one event occurs at a given location.

ment continues to the present comes from observed fault scarps in alluvial surfaces and relatively high seismicity (Sanford *et al.*, 1972).

Extensive volcanic activity, both inside and bordering the rift, has accompanied the formation of the structural depressions. In the Socorro area, many of the volcanics and associated intrusives of rhyolitic to andesitic composition are about 10 m.y. old (Weber, 1971). However, outpourings of basalt have continued up to very recent times. The compositions of recent flows in the Albuquerque-Socorro segment of the rift have not been studied. However, in the northern part of the rift in New Mexico, Lipman (1969) identified olivine tholeiites, a magma type that is believed to fractionate at shallow depths (15 to 20 km).

Numerous thermal springs along the entire length of the rift in New Mexico (Summers, 1965) are indicative of an abnormally high heat-flow beneath this structure. Recent heat-flow measurements along five profiles that cross the rift in New Mexico typically have the highest value near the rift (Edwards, Reiter, and Weidman, 1973). The highest heat-flow measurement to date in New Mexico, 11.5 HFU, was made in the mountains a few miles west of Socorro.

A structure of the length and character of the Rio Grande rift should have a deep-seated origin and, thus, anomalous upper mantle and crustal structure. Several observations, in addition to high heat-flow and thermal springs, indicate unusual conditions beneath the rift. In southern New Mexico, Warren *et al.* (1969) found thermal anomalies that could be correlated with the earlier discovery of a zone of high electrical conductivity underlying the rift. Lee and Borcherdt (1968) compared velocity spectra of the P_n phase at several distances and directions from the GASBUGGY underground nuclear explosion

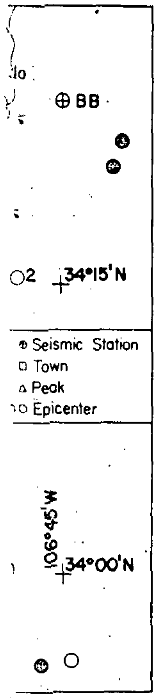

[illegible] 188 km north of Albuquerque. They found that the P_n phase was abnormally [illegible] for stations located in the rift. In an earlier paper, Jordan *et al.* (1965) reached a [illegible] conclusion on the basis of measured amplitude to period ratios.

[illegible] the other hand, some observations indicate nothing unusual about the rift structure. [illegible] measured P_n velocity between Socorro and Albuquerque is 8.1 km/sec, a value [illegible] typical of the Rocky Mountain States (Herrin, 1969). Phinney (1964), using a [illegible] based on the ratio of spectra of vertical and horizontal ground motion recorded [illegible] long-period instruments at Albuquerque (ALQ), obtained a crustal model with the [illegible] at a depth of 35 to 40 km and an intermediate discontinuity at 18 to 26 km. This [illegible] model is not greatly different from the one established in eastern New Mexico [illegible] the basis of Project GNOME data (Stewart and Pakiser, 1962).

Seismograph Stations and Records

[illegible] 1 shows the locations of stations providing data for this study, except for the [illegible] at Albuquerque (ALQ) which is 106 km N24E of SNM. Table 1 lists for each [illegible] (1) type of seismograph, (2) components recorded, (3) nominal magnification at [illegible], and (4) period of operation. Figure 2 shows the response curves for all seismo-[illegible] normalized to a magnification of 1.0 at 10 Hz.

TABLE 1

Characteristics and Period of Operation of Seismographs Used in the Study

[illegible]	System	Type of Recording	Components Recorded			Nominal Magnification at 10Hz	Period of Operation
			Z	NS	EW		
[illegible]	NMT	Pen and ink helical, at 4 mm/sec.	X			$1.3 \cdot 10^6$	7-1-61 to present
[illegible]	LRSM	Film (Benioff) and magnetic tape.	X	X	X	$6.0 \cdot 10^4$	6-8-69 to present
[illegible]	NMT	Helical film, at 1 mm/sec	X			$1.5 \cdot 10^5$	6-25-69 to 6-30-70
[illegible]	NOAA ASC-1	Magnetic tape with strip chart playback at 4 mm/sec.	X	X	X	$3.2 \cdot 10^5$	2-15-70 to 12-18-71
[illegible]	NOAA ASC-1	Magnetic tape with strip-chart playback at 4 mm/sec.	X	X	X	$1.2 \cdot 10^6$	2-26-70 to 11-29-71
[illegible]	WWSSN	Hot wire helical, at 1 mm/sec.	X	X	X	$2.0 \cdot 10^4$	10-3-61 to present

[illegible] 3 shows microearthquake seismograms recorded at stations SNM (NMT and [illegible] systems), CC (NOAA-ASC-1 system), and ALQ (WWSSN system). The late [illegible] phases used in this study are labeled 1 and 2. Phase 1 is generally not a well-[illegible] phase except on seismograms produced by the NMT system at station SNM [illegible] 3, a and b, and 9a). About 25 per cent of the close events ($S-P \leq 2.5$ sec) [illegible] by this vertical-component high-frequency response system (Figure 2) have an [illegible] phase 1 as well as phase 2. Phase 2 is clearly defined on about 40 per cent of [illegible] microearthquake seismograms at station SNM (NMT system), over 50 per cent of [illegible] horizontal-component seismograms at station BB, and over 90 per cent of the hori-[illegible] component seismograms at station CC. Phase 2 is very weak or nonexistent on [illegible] component seismograms at station SRM, which is located on a very thick section

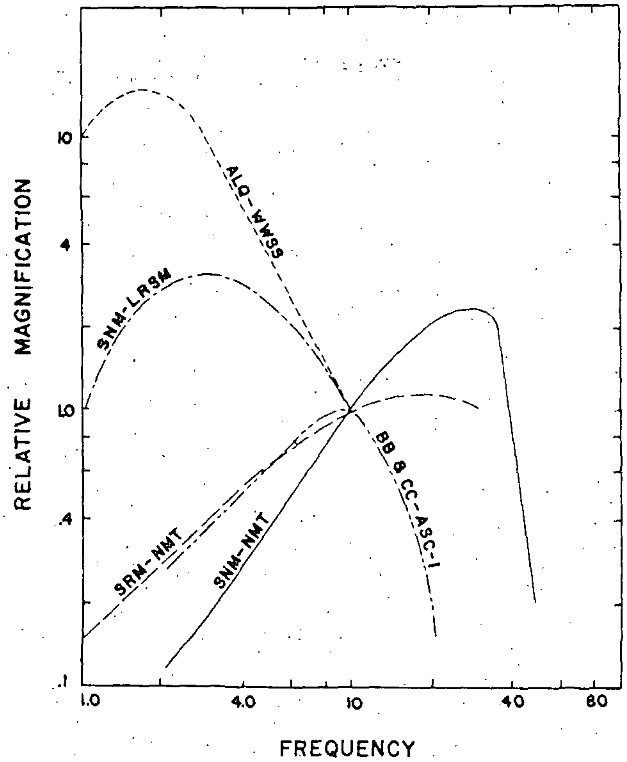

FIG. 2. Response curves for all seismographs used in the study. The curves have been normalized to a value of 1.0 at 10.0 Hz.

of low-velocity Tertiary alluvial fill (Santa Fe formation). Seismographs with high-frequency response appear to record phase 2 better than those with low-frequency response (compare the Z-component seismograms of the NMT system shown in Figure 3, a to f, with the Z-component records of the LRSM system shown in Figure 3, k and l).

Identification of Phases

Some conclusions about the nature of phase 2 can be obtained from an examination of the seismograms shown in Figure 3. First, this phase cannot result from peculiarities of station location or instrumentation, because it is well recorded at widely separated locations with seismographs of different instrumental characteristics. Second, phase 2 cannot be a surface wave because it has a sharp impulsive beginning and it is well recorded when the path between epicenter and station crosses a mountain range (Figure 3i). The elevation of the mountain range is many times greater than any reasonable estimate of wavelengths in phase 2. Third, the fact that phase 2 is strongest and most clearly defined on horizontal component instruments (Figure 3—i, k, and l) suggests that this phase contains S rather than P motion.

Graphs of travel times of phases 1 and 2 versus distance (S–P interval) suggest that these phases are reflections. Such a graph for data recorded by the NMT system at SNM is shown in Figure 4. In this figure, travel times for the two phases from each earthquake are plotted with the same symbol. Note that the absolute arrival times of phases 1 and 2 vary considerably for small changes in S–P, but the time difference between them

·es have been normalized to

Seismographs with hi[gh]
those with low-frequen[cy]
T system shown in Figu[re]
[sho]wn in Figure 3, k and l)

[obtai]ned from an examinati[on]
[migh]t result from peculiariti[es]
[reco]rded at widely separat[ed]
[charact]eristics. Second, pha[se]
beginning and it is w[ell]
mountain range (Figu[re]
[grea]ter than any reasona[ble]
[phase] 2 is strongest and m[ost]
[Figure] 3—i, k, and l) sugge[st]

[... S]$_{?}P$ interval) suggest th[at]
[t]he NMT system at SN[M]
[phas]es from each earthqua[ke]
[trave]l times of phases 1 and [2]
[d]ifference between the[m]

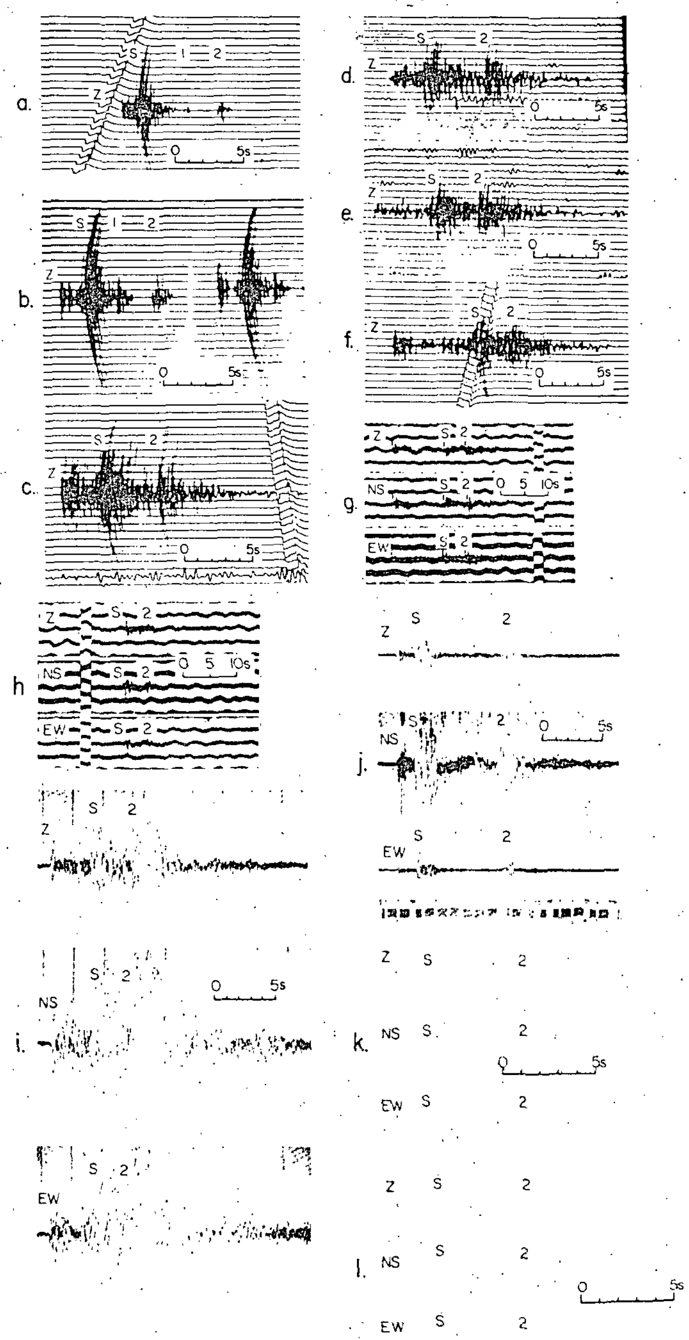

Fig. 3. Microearthquake seismograms showing reflections S_xP (phase 1) and S_xS (phase 2). Seismograms (a–f) were recorded by the NMT system at station SNM. Seismograms shown in (g) and (h) were recorded by the WWSS at ALQ. Seismograms shown in (i) and (j) were recorded by the ASC-1 system at station CC. Seismograms shown in (k) and (l) were recorded by the LRSM system at station SNM.

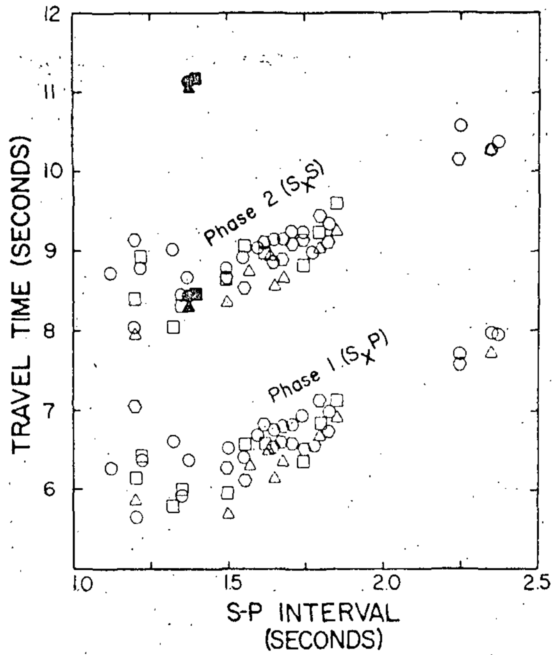

FIG. 4. Phase 1 (S_xP) and phase 2 (S_xS) arrival times versus $S-P$ interval. Travel times for the phases obtained from the same microearthquake have the same symbol. Data are from station SNM (NMT system).

phases for each event remains nearly constant. This observation can be explained if both phases are reflections and the depth of focus changes from event to event.

For the stations within 45 km of Socorro, no strong arrivals are observed that are later in time than phase 2. If this phase is a reflection, S_xS is the most promising candidate because it is the latest and potentially strongest of all the possible reflections. Phase 1, which is substantially weaker than phase 2, has arrival times that indicate it should be an S_xP reflection from the same discontinuity as the S_xS arrival. In Figure 5, differences between observed and theoretical arrival times for S_xP are plotted versus S-P

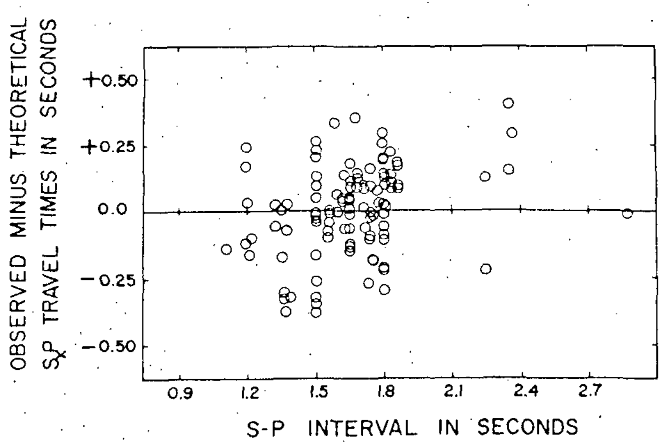

FIG. 5. Observed minus theoretical S_xP (phase 1) travel time versus $S-P$ interval. Theoretical values are based on a velocity discontinuity at a depth of 17.8 km. Data are from station SNM (NMT system).

intervals. Within the distance range $1.2 \leq S\text{–}P \leq 3.0$, the differences are remarkably small. It appears unlikely that such close agreement could be obtained unless phases 1 and 2 were actually S_xP and S_xS arrivals from the same discontinuity.

Additional evidence in support of identifying phase 2 as an S_xS reflection is obtained from an examination of amplitudes. Figure 6 shows the observed ratios of the amplitudes of phase 2 to direct P as a function of S–P. The data are from vertical-component seismograms (NMT system) at SNM. On the basis of the large values of these ratios,

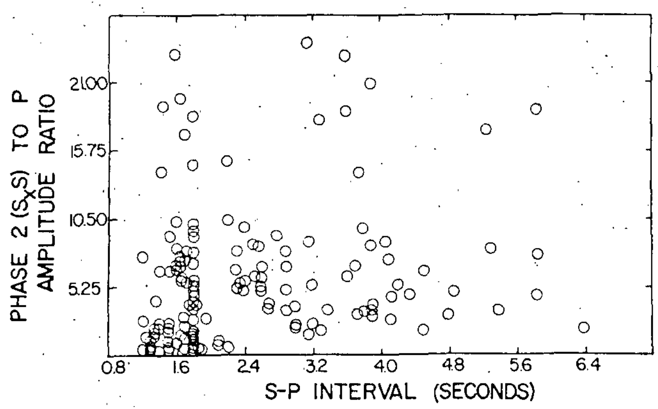

FIG. 6. Ratio of the amplitudes of phase 2 (S_xS) to direct P versus S–P interval. Data are from a vertical component instrument (NMT system) at SNM.

phase 2 cannot be a P_xP or a P_xS reflection. No reasonable combination of source mechanism, geometry of source relative to station, or conditions at a velocity discontinuity could produce a P_xP (or P_xS) phase 5 to 10 times stronger than the direct P phase. A correction for angle of incidence will not improve the situation. At station SNM, the direct wave also arrives at a steep angle, generally 15° to 20° with respect to the vertical, because of low-velocity rock directly beneath the station.

Figure 7 shows the observed ratios of the amplitudes of phase 2 to direct S. Data are again from vertical-component seismograms (NMT system) taken at station SNM. The

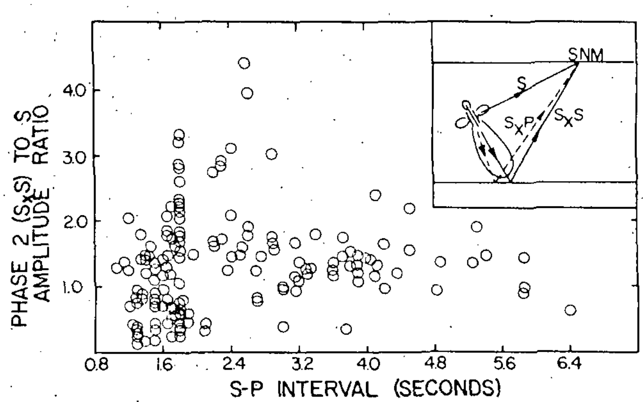

FIG. 7. Ratio of the amplitudes of phase 2 (S_xS) to direct S versus S–P interval. Data are from a vertical component instrument (NMT system) at SNM.

...gions like the Rio Gra...
...able mechanism for mi...
...agating unilaterally do...
model, the S-wave ...
...d from the focus (see ...

...line between the focus ...
...ing station. For a refle...
...e ray path for the refle...
...ult axis and the ray ...
...e surface. Some indic...
... directions from the fa...
amplitudes of first ...
...d velocity of rupture...
0.9 times the shear...
...ll be 10 times greater...
... S wave following the...
...r than the signal follo...

S wave because it ...
...g and attenuation. ...
S_xS to S also depe...
base of normal ...
...ndicate that the ...
...ially greater. Taking ...
...veled, and coeffici...
...e model. A ratio of ...
...own in this figure ...
...ification of S_xP and ...
...rect S, particularly ...
...es at large S–P ...
... are biased toward ...
respect to the stati...

...ing discontinuity ...
... material above ...
...ned originally ...
...uakes accurately ...
...the travel time of ...

...om station SNM ...
were searched fo...
...lected event, ...
depth of focus ...
...sults of the calcu...
... obtained by ...
...e, the depth of ...

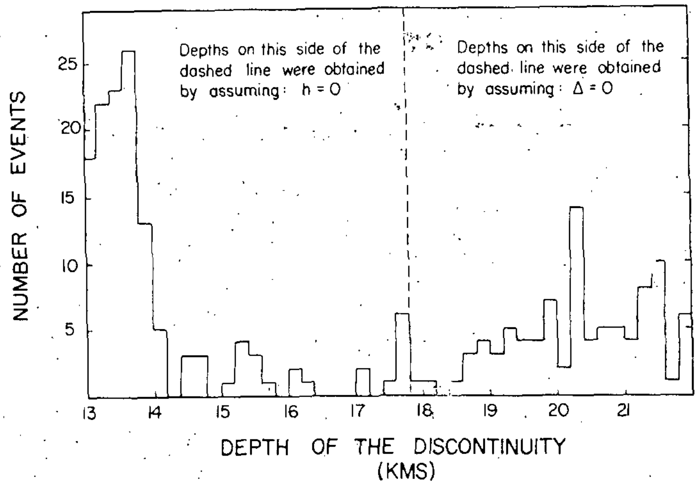

...8. Depth of the discontinuity using data from station SNM only. Basic data used were (1) S–P ...ation of P–O and distance to focus and (2) S_xS-O for calculation of the depth of the dis-...

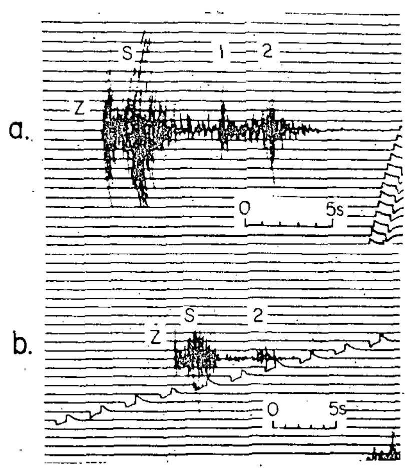

...ismograms of microearthquakes with a depth of focus near zero (a) and an epicentral distance near zero (b).

...ity beneath station SNM is 17.8 km. Seismograms for earthquakes nearly having ...ed conditions, i.e., $h = 0$ or $\Delta = 0$, are shown in Figure 9.

...depths to the reflecting discontinuity at points near Socorro were obtained by ...flection data generated by some of the earthquakes located in Figure 1. Depth ...ons were restricted to shocks that produced clearly defined S_xS phases and that ...d to have accurate hypocenters. Results are shown in Figure 10, where depth ...re plotted at the reflection points (circles) and depths of focus are given at the ...s (squares). The most consistent results appear to be southwest of SNM where ...aving quite different focal depths yield very nearly the same depths to the ...uity. Elsewhere, the scatter in depths is believed to be the result of errors in the ...focus.

...depths, given in Figure 10, indicate that the discontinuity is dipping northward ...corro. Other data appear to confirm this observation. On Figure 11 are plotted ...d times at SNM out to an S–P distance of 6.4 sec. Shocks known to have very ...depths of focus have been deleted from this graph. A good theoretical fit to the ...S_xS reflection times requires that the discontinuity dip approximately 6°.

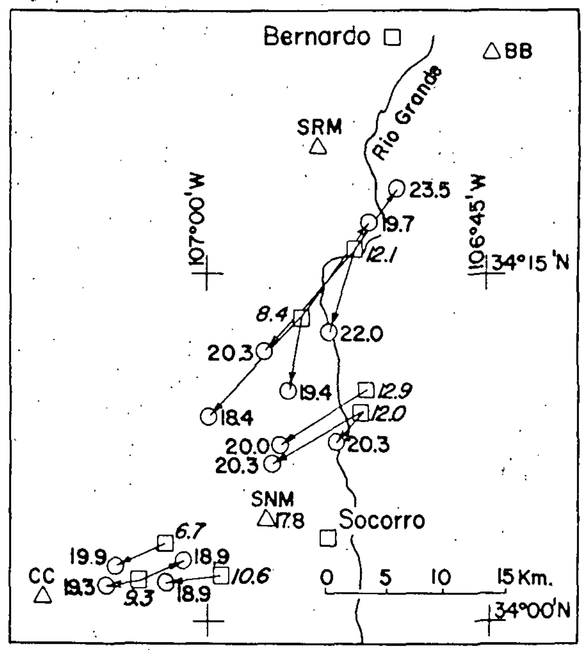

FIG. 10. Map showing depth of the discontinuity in the vicinity of Socorro. Discontinuity depths are given at the reflection points (circles) and focal depths are given at the epicenters (squares).

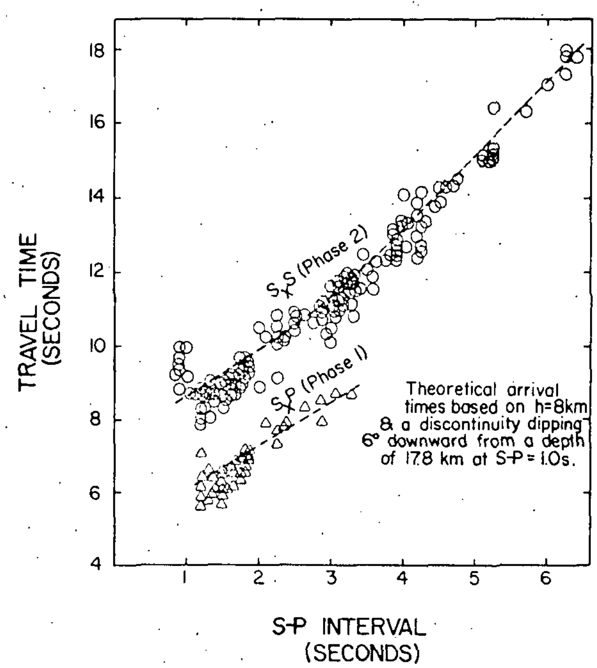

FIG. 11. Travel times of S_xP (phase 1) and S_xS (phase 2) versus $S-P$ interval. Data are from station SNM (NMT system).

...ution of epicenters shown in Figure 1 indicates that most of the reflection ...ances of $S–P \geqq 2.0$ are from shocks located north of Socorro. Therefore, ...es of dip required to match the observations must be northward. The depth of ...d for the theoretical curve in Figure 11, $h = 8$ km, is the average depth calcu... the S_xS arrival times (for events with $S–P \leqq 2.0$) assuming a depth to the ...interface of 17.8 km.

...ections are observed on ALQ seismograms of earthquakes occurring near ...(Figure 3, g and h). The reflection times from these records were used to map ...tinuity northward along the Rio Grande rift. Results of these calculations are ...Figure 12. Only shocks whose epicentral distances and depths of focus were ...to be known within 2 and 4 km, respectively, were used in these calculations.

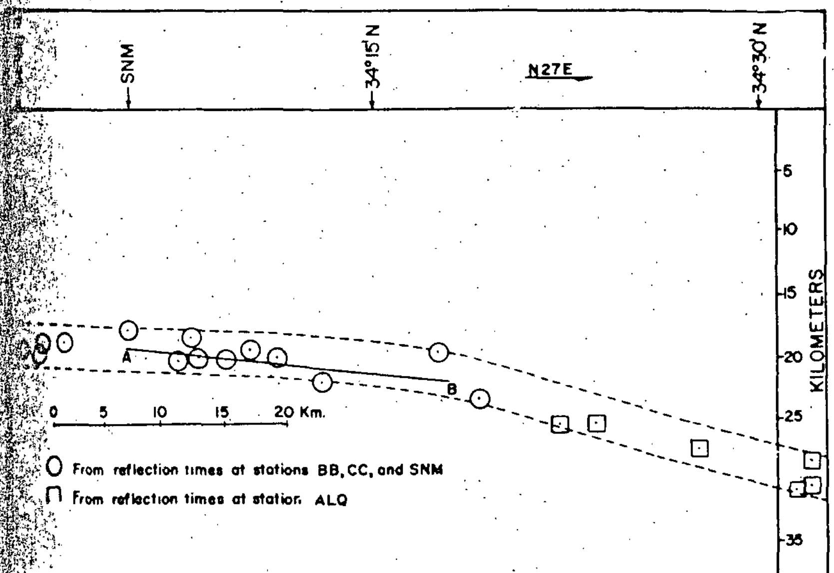

...2. Depths of discontinuity along a profile oriented N27E from Socorro to Albuquerque.

...to these parameters, the calculated depths at large distances depend critically ...ce of velocity. For example, a change in S-phase velocity from 3.34 to 3.42 ...4 per cent) changes the calculated depth of the discontinuity by 2.3 to 4.5 km ...tral distances ranging from 80 to 120 km. No measurements made during this ...d be used to determine the S velocity along the reflection path with a precision ...per cent. Therefore, a constant velocity was selected that produced the smoothest ...in depths from the Socorro area northward. This velocity, 3.38 km/sec, was ...less than that measured for the direct S, 3.48 km/sec. However, the standard ...on the latter measurements was 0.07, and, therefore, little significance should ...d to the difference in velocities.

Properties of the Discontinuity

...km-deep discontinuity beneath Socorro must be sharp because S-phase ...aining high-frequency oscillations are readily and apparently preferentially ...om it (Figure 3). Also, the generally large amplitude of S_xS reflections suggests ...l difference in S-phase velocity across the discontinuity.

...that plane-wave reflection theory is applicable, the ratio of S_xP to S_xS

amplitudes as a function of distance can be used to estimate the velocity contrast at the discontinuity. S_xP and S_xS are generated by S-phase energy traveling along separated ray paths from the focus, and, thus, their amplitude ratio is relatively unaffected by differences in radiated energy from the focus. Table 2 lists five S_xP to S_xS amplitude ratios, each obtained by averaging many observed ratios narrowly grouped about the tabulated angles of incidence. The data for these ratios were obtained from a vertical component instrument (NMT system) at SNM. The measured amplitudes have been corrected by multiplying by the sine of the angle of incidence for the S_xS wave and dividing by the cosine of the angle of incidence for the S_xP phase.

Theoretical amplitude ratios of S_xP to S_xS, based on plane-wave theory, are presented in Table 2 for the same angles of incidence as the observed ratios. For a 3.46-to-0 km/sec S-wave velocity contrast across the discontinuity, the theoretical ratio is greatly different from the observed ratios, particularly when the angle of incidence for S_xS is near 20°. Theoretical ratios more in agreement with observed ratios are obtained by postulating a 50 per cent decrease in S-wave velocity from the surface to the discontinuity. However, theoretical ratios as high as 1.27 are still obtained. In addition, the velocity calculated for S-wave reflections from Socorro to Albuquerque does not appear to support this crustal model.

Another way to make theoretical values agree more closely with observed values is to have a discontinuity across which the S-wave velocity drops to zero and the P-wave velocity remains the same. This approximates the boundary between rigid and nonrigid layers having different compositions. The theoretical values for this case, listed in Table 2, still exceed the observed values, but the discrepancy is greatly reduced. In addition, the steady increase in the observed ratios with increase in angle of incidence is duplicated with this type of discontinuity.

Slightly better agreement between theoretical and observed values of the amplitude ratio S_xP/S_xS is obtained when the P-wave velocity increases from 6.0 to 8.0 km/sec and the S-wave velocity decreases from 3.46 to 0.0 km/sec across the discontinuity. However, this model appears unsuitable because nonrigid material of petrologically reasonable composition will have a velocity much less than 8.0 km/sec. This consideration, as well as the observed amplitude ratios, indicates that the discontinuity is underlain by low-rigidity material having a P-wave velocity little different from the overlying material. If this interpretation is correct, the 18-km discontinuity could not be the Moho because the P velocity below this discontinuity would be far smaller than the observed P_n velocity. The position of the Moho could be anywhere from a fraction of a kilometer to many kilometers deeper than the 18-km discontinuity. The fact that no phases are observed later than the S_xS reflection from the 18-km discontinuity (Figure 3) does not rule out the possibility of a much deeper first-order discontinuity. Strong reflections later than S_xS would not exist because almost all of the S-phase energy would be reflected at the 18-km discontinuity. Reflections of a totally P-wave character from a deeper discontinuity would probably be too weak to be identified.

CONCLUSIONS

The important characteristics of the crustal discontinuity beneath the Rio Grande rift near Socorro are summarized below:

1. The depth directly beneath Socorro is about 18 km.
2. The discontinuity dips northward and obtains a depth near 30 km at a distance of 60 km from Socorro.
3. The discontinuity is sharp and could be underlain by material of very low rigidity.

the velocity contra[illegible]
energy traveling [illegible]
tude ratio is relati[illegible]
ble 2 lists five S_xP [illegible]
d ratios narrowly [illegible]
tios were obtained [illegible]
measured amplitud[illegible]
of incidence for [illegible]
S_xP phase.
wave theory, are [illegible]
ratios. For a 3.46 [illegible]
the theoretical [illegible]
the angle of incide[illegible]
h observed ratios [illegible]
locity from the [illegible]
.27 are still obta[illegible]
Socorro to Alb[illegible]

with observed val[illegible]
to zero and the [illegible]
etween rigid and [illegible]
this case, listed [illegible]
tly reduced. In a[illegible]
of incidence is d[illegible]

values of the [illegible]
from 6.0 to 8.0 [illegible]
across the dis[illegible]
aterial of [illegible]
km/sec. This [illegible]
e discontinuity [illegible]
rent from the [illegible]
y could not be the [illegible]
naller than the [illegible]
fraction of a [illegible]
fact that no [illegible]
nity (Figure 3) [illegible]
Strong reflect[illegible]
y would be [illegible]
acter from a [illegible]

neath the Rio [illegible]

30 km at a [illegible]

of very low [illegible]

TABLE 2

Observed and Theoretical Ratios of S_xP to S_xS Amplitudes

Observed			Theoretical					
			$\alpha_1 = 6.00$, $\beta_1 = 3.46$	$\alpha_2 = 8.00$, $\beta_2 = 4.60$		$\alpha_1 = 5.80$, $\beta_1 = 3.35$	$\alpha_2 = 5.80$, $\beta_2 = 0.00$	
Angle of Incidence S_xS	Measured S_xP/S_xS Ave. ± S.D.	Corrected S_xP/S_xS Ave. ± S.D.	Reflection Coefficient P^*	Reflection Coefficient S^*	Ratio	Reflection Coefficient P	Reflection Coefficient S	Ratio
8.8	0.11 ± 0.023	0.017 ± 0.0035	0.05	0.18	0.28	0.12	0.94	0.13
17.3	0.15 ± 0.057	0.046 ± 0.017	0.09	0.09	1.0	0.22	0.82	0.27
21.1	0.24 ± 0.20	0.088 ± 0.074	0.10	0.03	3.3	0.25	0.75	0.33
23.3	0.27 ± 0.22	0.111 ± 0.086	0.11	0.04	2.7	0.27	0.72	0.38
30.5	0.58 ± 0.10	0.314 ± 0.056	0.12	0.18	0.67	0.32	0.67	0.48

[illegible] McCamy *et al.* (1962).

[illegible] discontinuity could be related to some unusual features of the Rio Grande rift in [illegible]ity of Socorro. A characteristic of rift structure near Socorro is intergraben [illegible] These horsts are narrow fault block mountains that extend northward from Socorro [illegible]ance of about 20 km. They formed relatively late in the history of the rift, i.e., [illegible] downdropping and sedimentary filling of a relatively large graben structure (Denny, [illegible] The fact that intergraben horsts exist near Socorro but not northward in the rift [illegible] related to the shallow depth of the crustal discontinuity at Socorro. A shallow [illegible]uity underlain by hot material of low rigidity could also explain the high heat-[illegible] mountains a few kilometers west of Socorro.

Acknowledgments

[illegible]arch described in this paper was supported by the National Science Foundation through [illegible]30767. We wish to acknowledge the Albuquerque Seismological Center (ERL, NOAA) for [illegible] in the form of equipment and data.

References

[illegible] C. E. (1971). The Rio Grande rift, Part 1: Modifications and additions, *New Mexico, Geol. Soc. [illegible]ook, 21st Field Conf.*, 191–201.

[illegible] S. (1941). Quaternary geology of the San Acacia area, New Mexico, *J. Geol.* **49**, 225–260.

[illegible] C. L., M. A. Reiter, and C. Weidman (1973). Geothermal Studies in New Mexico and Southern [illegible] (*abstract*), *Trans. Am. Geophys. Union* **54**, 463.

[illegible] W. (1963). Structural geology of the Little San Pasqual Mountain and the adjacent Rio [illegible] trough, *M.S. Thesis*, New Mexico Institute of Mining and Technology, Socorro, New [illegible]

[illegible] (1969). Regional variations of *P*-wave velocity in the Upper Mantle beneath North America, [illegible] *Geophys. Union Mon.* **13**, 242–246.

[illegible] H. R., J. E. Case, and L. E. Cordell (1961). The Rio Grande near Albuquerque, New Mexico, [illegible] *Mexico Geol. Soc. Guidebook, 12th Field Conf.*, 148–150.

Jordan, J., R. Black, and C. C. Bates (1965). Patterns of maximum amplitudes of P_n and P waves over regional and continental areas, *Bull. Seism. Soc. Am.* **55**, 693–720.
Kelley, V. C. (1952). Tectonics of the Rio Grande depression of central New Mexico, *New Mexico Geol. Soc. Guidebook, 3rd Field Conf.*, 93–105.
Kelley, V. C. (1956). The Rio Grande depression from Taos to Santa Fe, New Mexico, *New Mexico Geol. Soc. Guidebook, 7th Field Conf.*, 109–114.
Lee, W. H. K. and R. D. Borcherdt (1968). P_n-spectral variations of the Gasbuggy explosion at intermediate distance ranges, *USGS Open File Report, Tech. Letter NCER-9*, 18 p.
Lipman, P. W. (1969). Alkalic and tholeiitic basaltic volcanism related to the Rio Grande depression, southern Colorado and northern New Mexico, *Bull. Geol. Soc. Am.* **80**, 1343–1354.
McCamy, K., R. P. Meyer, and T. J. Smith (1962). Generally applicable solutions of Zoeppritz amplitude equations, *Bull. Seism. Soc. Am.* **52**, 923–955.
Phinney, R. A. (1964). Structure of the Earth's crust from spectral behavior of long-period body waves, *J. Geophys. Res.* **69**, 2997–3017.
Sanford, A. R. (1968). Gravity survey in central Socorro Country, New Mexico, *New Mexico State Bur. Mines and Mineral Resources, Circ. 91*, 14 p.
Sanford, A. R. and L. T. Long (1965). Microearthquake crustal reflections, *Bull. Seism. Soc. Am.* **55**, 579–586.
Sanford, A. R., A. J. Budding, J. P. Hoffman, O. S. Alptekin, C. A. Rush, and T. R. Toppozada (1972). Seismicity of the Rio Grande rift in New Mexico, *New Mexico State Bur. Mines and Mineral Resources, Circ. 120*, 19 p.
Savage, J. C. (1965). The effect of rupture velocity upon seismic first motions, *Bull. Seism. Soc. Am.* **55**, 263–275.
Stewart, S. W. and L. C. Pakiser (1962). Crustal structure in eastern New Mexico interpreted from the Gnome explosion, *Bull. Seism. Soc. Am.* **52**, 1017–1030.
Summers, W. K. (1965). A preliminary report on New Mexico's geothermal energy resources, *New Mexico State Bur. Mines and Mineral Resources, Circ.* **80**, 41 p.
Warren, R. E., J. G. Schlater, V. Vacquier, and R. F. Roy (1969). A comparison of terrestrial heat flow and transient geomagnetic fluctuations in the southwestern U.S., *Geophysics* **34**, 463–478.
Weber, R. H. (1971). K-Ar ages of Tertiary igneous rocks in central and western New Mexico: *Isochron/West 71-1*, 33–45.

Department of Geoscience
New Mexico Institute of Mining and Technology
Socorro, New Mexico 87801

Manuscript received May 4, 1973